

## Molecular-dynamical study of second sound in a solid excited by a strong heat pulse\*

D. H. Tsai and R. A. MacDonald

*National Bureau of Standards, Washington, D. C. 20234*

(Received 13 May 1976)

We use the method of molecular dynamics to study the problem of heat transfer in a perfect semi-infinite bcc lattice when a strong heat pulse is applied at the boundary. We find that the disturbance propagates into the lattice as a combination of first sound and second sound superimposed on a diffusive background. The second-sound wave is a composite of several waves. We are able to show that the longitudinal and transverse sound waves, traveling with velocity  $C_l$  and  $C_s$ , respectively, are generated by the disturbance when the boundary of the lattice is rapidly heated or cooled. These stress-induced pulses are not in thermal equilibrium but they generate their own temperature waves, which travel with velocities  $C_l/\sqrt{3}$  and  $C_s/\sqrt{3}$ , and which contribute to the observed second-sound wave. The disturbance in kinetic energy produced during the period of steady heating in the pulse propagates as a temperature wave with the theoretically expected second-sound velocity,  $C_{sv}/\sqrt{3}$ . We relate these results to theoretical and experimental work on second sound excited by a weak pulse and also to our earlier calculations where the temperature wave is excited by shock compression.

### I. INTRODUCTION

In recent years we have been developing our capability to use the method of molecular-dynamical calculation to study the motion of atoms in a crystalline lattice under nonequilibrium conditions. This method has been used extensively, and with great success, in the study of thermodynamic<sup>1</sup> and transport<sup>2</sup> properties of solids and liquids. Much of this work has been concerned with the exact calculation of quantities, generally phase averages, which appear in statistical-mechanical theories of anharmonic systems and which could not be calculated without approximation by other methods. This is certainly a valid use of molecular dynamics. However, there are other features of the method which we wish to utilize. For example, the numerical solutions contain such extraordinary details of the atomic motions that it is possible to observe directly the mechanism and the evolution of atomic processes. Moreover, with complete and precise control over the initial and boundary conditions, the effect of a change in these conditions on the problem under study may be determined unambiguously. In fact, this control enables one to modify the initial and boundary conditions of the molecular-dynamical system so that with very little additional effort a wide range of experimental situations may be simulated. Further, it is most important for our interest in the high-pressure high-temperature regime that anharmonic effects are fully included, with no approximation.

In this paper we describe our use of the molecular-dynamical method to make a detailed analysis of energy transport in a dielectric crystal subjected to intense pulsed heating. This problem is undoubtedly of practical importance in laser pellet

implosion experiments where temperature plays a crucial role. It is also important in the development of radiation standards and in the measurement of thermophysical properties of dense systems. In the study of second sound in a solid, heat-pulse experiments have customarily been limited to weak pulses and low temperatures.<sup>3,4</sup> These limitations have arisen partly from theoretical and partly from experimental considerations. Theoretically, the second-sound mode can be derived either as a solution of the phenomenological Boltzmann equation<sup>5</sup> or as a natural mode of the displacement correlation function.<sup>6,7</sup> In both cases it is assumed that the departure from thermal equilibrium is very small in order that a linear approximation may be made. Consequently, a very weak heat pulse is required. Experimentally, a low temperature and a very pure sample are necessary if the second-sound wave is not to be damped out by dissipative scattering processes. Whether the experimental situation meets other requirements of second-sound theory such as negligible thermoelastic coupling, it is hard to say. Certainly some difficulty arises in relating experiment to theory. For example, theory gives either a constant second-sound velocity  $V_{II}$ ,<sup>5</sup> or a temperature-dependent second-sound velocity with  $V_{II}$  as the maximum value.<sup>8</sup> But experimentally, the second-sound velocity shows no sign of tending to  $V_{II}$ . At low temperatures, it tends toward the transverse sound velocity  $C_s$  (greater than  $V_{II}$ ), and as the temperature is raised, it decreases continually until the signal is lost in the diffusive background. Also, the first-sound pulses, attributed to "ballistic" phonons,<sup>3</sup> are much larger than those predicted by theory for the first sound generated by a heat pulse.<sup>7</sup> In our computer "experiment," we have

such control over the situation that we are in an advantageous position to obtain clear unambiguous results. For example, there is no impurity scattering in the perfect crystal, there is no problem of impedance mismatch at the heater-crystal interface, and there is constant monitoring of both stress and temperature along the whole length of the lattice. Although we use a strong heat pulse, we expect that the understanding gained from our results should give insight into the weak-heat-pulse problem also. In addition, the strong heat pulse is relevant to our earlier work on shock-wave propagation.<sup>9,10</sup> There, we observed that the thermally equilibrated region behind the shock front propagated as a wave with velocity less than that of the shock front. We identified this temperature wave with second sound in the high-pressure high-temperature regime. To our knowledge, molecular dynamics provides the only practicable method for studying problems in this highly anharmonic regime.

We gave a preliminary report of this work in Ref. 11. Here we present a full report of our calculations. In Sec. II we describe the model used to simulate a solid subjected to a heat pulse. In Sec. III we give a brief summary of the theory needed to analyze our earlier results<sup>12</sup> for the diffusive flow by steady heating of a lattice at a moderate temperature. This calculation is important since it tests our molecular-dynamical model and shows it to be realistic. We use this theory to delineate the diffusive contribution to the heat pulse. We present and discuss our results in Sec. IV. A summary is given in Sec. V.

## II. LATTICE MODEL, INITIAL AND BOUNDARY CONDITIONS

Most of this work has been carried out for the three-dimensional bcc lattice. The lattice model is shown in Fig. 1: a semi-infinite lattice is made up of cubes of 125 ( $5 \times 5 \times 5$ ) bcc unit cells joined together with cyclic boundary conditions on opposite faces. The edges are aligned with the Cartesian-coordinate directions  $x, y, z$ . The free surface is at  $z = 0$ . This division into cubes saves computation time, since one such cube is typical of the undisturbed lattice in thermal equilibrium. Heat is added (see below) at the free surface, where the boundary condition is mirror reflection. As the disturbance propagates into the lattice in the  $+z$  direction, the cyclic boundary condition in that direction is progressively removed, cube by cube, up to the point reached by the disturbance. At this point the disturbed lattice is joined smoothly to the undisturbed lattice. Thus, we consider a "typical" filament of the semi-

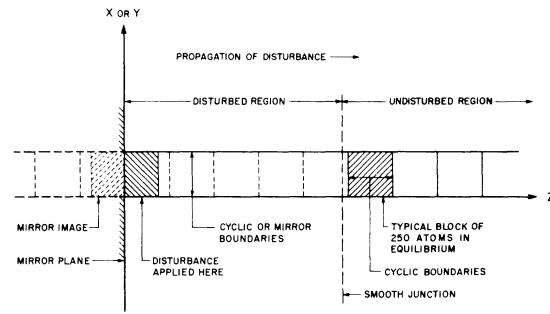


FIG. 1. Lattice model.

infinite lattice and calculate its response to heating at the boundary ( $z = 0$ ). The filament has a cross section of 25 unit cells with 25 lattice points per plane. We have allowed the disturbance to propagate to a maximum of 500 lattice planes (12 500 atoms in the filament).

We have also imposed mirror boundary conditions on the transverse boundaries of the filament (in the  $\pm x, \pm y$  directions). The reason for changing to these boundary conditions is as follows: in the calculation of diffusive heat flow<sup>12</sup> we observed a twofold increase in the lattice energy above that actually on record as added to the system during the calculation. This problem had to be resolved or the validity of all our previous results would have been in question. We discovered that the cyclic boundary condition allowed the lattice filament to drift laterally from its equilibrium position due to small truncation and round-off errors in our calculation. However, the undisturbed end of the lattice was held in place. Thus, the drift was not uniform along the length of the filament. This caused the lattice to distort and strain energy to build up. With mirror boundary conditions in the transverse directions, the filament is constrained to stay in place, so no strain energy is developed. The energy of the system is now satisfactorily conserved.

We have also studied the two-dimensional lattice to verify the change in second-sound velocity predicted by theory. In this case, the bcc unit cells form a ribbonlike filament placed on Cartesian coordinates with 25 units in the  $x$  direction and one unit in the  $y$  direction. Two-dimensional motion is obtained by requiring zero motion in the  $y$  direction. Cyclic or mirror boundary conditions are imposed as in the three-dimensional case.

For thermal equilibrium, we require that the velocity distribution of the atoms be Maxwellian with equipartition of kinetic energy in the  $x, y,$  and  $z$  degrees of freedom and that the energy density of the lattice be constant. Under these conditions, the kinetic temperature of the lattice is

defined as

$$T = (m/3k)\langle v_x^2 + v_y^2 + v_z^2 \rangle,$$

where  $m$  is the mass of an atom;  $v_x, v_y, v_z$  are the Cartesian components of its velocity;  $\langle \dots \rangle$  indicates an average over all atoms in the system; and  $k$  is Boltzmann's constant. To simulate thermal equilibrium, the lattice atoms, initially in their static equilibrium positions, are randomly assigned a Maxwellian velocity distribution for each degree of freedom and the dynamics of the system is allowed to evolve. The energy of the system is monitored continuously. In this system of closely coupled atoms, the exchange between kinetic and potential energy takes place very rapidly, and when motion is initiated in the manner described here, we find that thermal equilibrium is established within two or three atomic oscillations. This means that we can also change the temperature of the system simply by applying a scaling factor to the velocity components of all the atoms. If the adjustment is small compared with the fluctuations the condition of local thermal equilibrium is not significantly disturbed.

To initiate the heat pulse, the first ten ( $x$ - $y$ ) lattice planes are heated rapidly from their initial equilibrium temperature,  $T_i$ , at time  $\tau=0$ , to an average temperature  $T_h$  by scaling the velocities of the atoms in these planes. Then, the end of the heat pulse is signalled by rapid removal of heat in such a way that at  $\tau=\tau_h$ , the temperatures of the ten planes has dropped to a temperature  $T_1$ . This removal of heat does not occur in the laboratory experiment. It affects the shape of the heat pulse, but should not affect our interpretation of the results. After  $\tau=\tau_h$ , the system is left to itself (no heat added nor removed) and the calculation proceeds until the pulse reaches the 500th plane of the lattice or a suitable earlier stopping point.

Under all the various combinations of the conditions above, the computational procedure is the same: we solve the classical equations of motion for the lattice atoms by numerical integration to yield the position and velocity of each atom. The average kinetic energy, potential energy, stress components, and density of lattice planes are obtained as functions of time. These results show the transport of energy into the lattice. The interatomic potential used is that constructed by Chang<sup>13</sup> for the lattice of  $\alpha$ -iron. Since we are only interested in the qualitative rather than the quantitative behavior of the system, the actual potential used is not important for our present purposes, provided it represents a stable lattice structure. We use the iron potential just for our convenience.

To demonstrate the versatility of the model, we note first that shock-wave propagation is effected simply by changing the boundary condition at the free surface from that of heating the first ten lattice planes to that of impact between the semi-infinite lattice and its mirror image across the plane  $z=0$ , as described in Ref. 10. Further, two-dimensional wave propagation is effected by setting the values of the  $y$  components of atomic displacement and velocity equal to zero. Finally, the change from heat pulse to steady heating (for the thermal diffusivity problem<sup>12</sup>) is accomplished by maintaining the temperature of the heated planes at  $T_h$  for the rest of the calculation.

### III. ANALYSIS OF DIFFUSIVE HEAT FLOW

We first summarize our results for diffusive heat flow by steady heating of a lattice at moderate temperature.<sup>12</sup> This is one case where we should simulate the experimental situation well and thus have a definitive test of our model, viz., that heat flow is indeed diffusive at this temperature (44 K), and that the thermal diffusivity has a reasonable value. We used a two-dimensional model to shorten computation time. We obtain the diffusive temperature profile  $T(z, \tau)$  appropriate to our initial and boundary conditions from the theory of diffusive heat flow.<sup>14</sup> We determined the thermal diffusivity  $\alpha$ , and hence the scale of  $T(z, \tau)$ , by fitting these results to the computed temperature profile at one time. We obtained the value,

$$\alpha = 4.0 \times 10^{-6} \text{ m}^2 \text{ sec}^{-1}.$$

Using this value of  $\alpha$ , the  $T(z, \tau)$  at other times fitted the computed profiles well and their energy content was found to be in good agreement with that recorded as added to the system. Whether  $\alpha$  has a reasonable value is harder to answer since we cannot obtain a truly experimental value for the lattice contribution to thermal diffusivity (or thermal conductivity, the quantity usually measured). A "best estimate"<sup>15</sup> for the lattice thermal conductivity of the alloy  $\text{Fe}_{99.5}\text{Ni}_{0.5}$  at 75 K is

$$\kappa = 28.2 \text{ W m}^{-1} \text{ K}^{-1},$$

whereas our value of  $\alpha$  for pure Fe gives

$$\kappa = 9.4 \text{ W m}^{-1} \text{ K}^{-1}.$$

Considering the fact that the effective interatomic potential for iron is not known at all accurately, we feel that the agreement obtained here is satisfactory. We conclude from these results that the molecular-dynamical model exhibits diffusive flow and is indeed realistic.

In the case of heat-pulse propagation there is

evidently a diffusive contribution to the heat flow even for a lattice initially at absolute zero. We wish to estimate this contribution not only to set off the temperature wave from the diffusive background but also to show that, ultimately, the drop in temperature at the boundary is controlled by diffusion. We cannot solve the diffusive heat flow equation analytically in this case since the initial and boundary conditions are too complex. Instead, we obtained the solution by a finite-difference method.<sup>16</sup> If  $T_{mn}$  denotes the temperature at a distance  $m\Delta z$  from any starting point and at a time  $n\Delta t$  from any time origin, and if we choose values of  $\Delta z$  and  $\Delta t$  such that the thermal diffusivity is given by

$$\alpha = \frac{1}{2}(\Delta z)^2/\Delta t,$$

then the temperature profile at the next time step is given by

$$T_{m,n+1} = \frac{1}{2}(T_{m+1,n} + T_{m-1,n}).$$

The temperature profiles for later times  $\tau$  are generated by this equation from some arbitrary starting point at  $\tau_1 > \tau_h$ , subject to the condition that

no heat is added at the boundary. We shall discuss how the fit is achieved in Sec. IV.

#### IV. RESULTS

In this section, we present the results for heat pulse propagation into a three-dimensional lattice at 0 K using mirror boundary conditions. The heat pulse is applied by heating the first ten lattice planes to a temperature  $T_h \approx 800$  K (twice the Debye temperature) for the period  $0 < \tau < 40$ , where  $\tau$  is measured in units of  $d/C_l$ , the ratio of interplanar spacing to longitudinal sound velocity (equal to  $0.264 \times 10^{-13}$  sec). Both the addition and removal of heat, at the beginning and end of this period respectively, are rapid, taking place over two time units. In Fig. 2 we show the evolution of the kinetic temperature profile, labeling the significant waves that propagate into the lattice. Each point used to construct these profiles represents an average about that point over 15 lattice planes and two units of time. Figures 3–5 help us analyze these results. The labels correspond to those given in Fig. 2. In Fig. 3 we have selected five

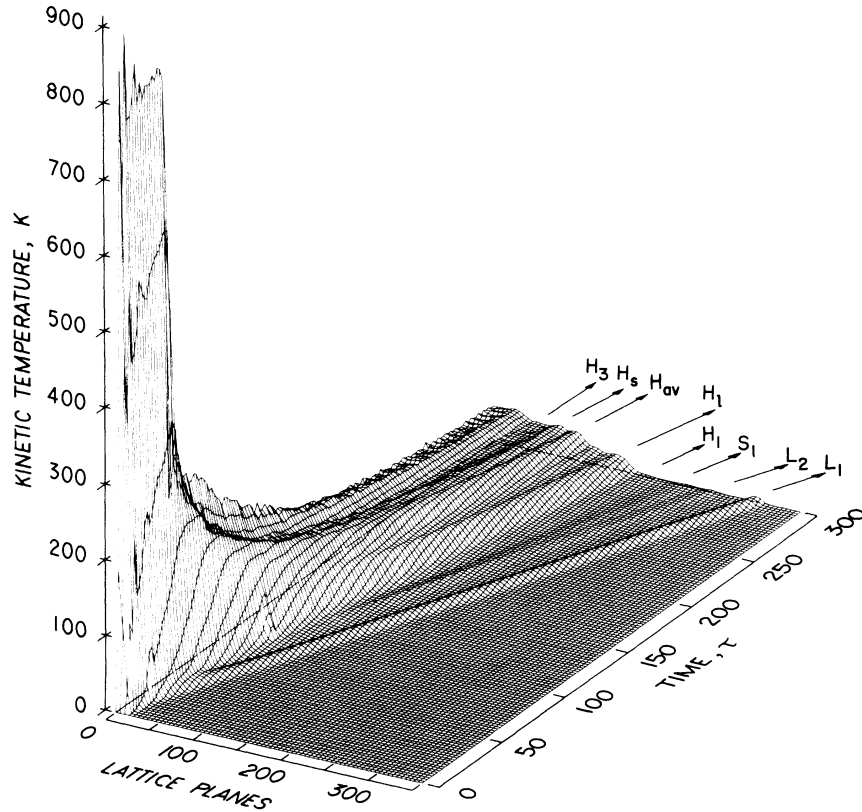


FIG. 2. Evolution of kinetic temperature profile ( $K$ ) as a function of lattice plane number and time  $\tau$  for  $T_i=0$  K, mirror boundary conditions, three dimensional lattice.  $L_1$ ,  $L_2$ ,  $S_1$ ,  $H_1$ ,  $H_1$ ,  $H_{av}$ ,  $H_s$ , and  $H_3$  label features in the profile moving with constant velocity to be discussed in the text.

kinetic temperature profiles, omitting the time averaging, for a more detailed examination of the various features in Fig. 2. In Fig. 4, we plot the  $x$ ,  $y$ , and  $z$  components of kinetic temperature and the longitudinal component of stress as a function of lattice plane number at  $\tau = 300$ . The points represent an average over 15 lattice planes as before, but now the time average is taken over four units. We make use of this figure to consider the question of local thermal equilibrium in the heat pulse. In order to compare our results with those of heat-pulse experiments,<sup>3</sup> in Fig. 5(a) we show time profiles of the kinetic temperature from a given standpoint, station 15 (average of planes 71 to 75) in the lattice. The three profiles are for (A)  $T_i = 0$  K and (B)  $T_i = 38$  K, both with cyclic boundary conditions and (C)  $T_i = 0$  K with mirror boundary conditions. In Fig. 5(b) we construct the limiting wavefronts for our particular initial and boundary conditions to aid the discussion and interpretation of the results, as in Ref. 11.

We now return to Fig. 3. The dashed lines show the trajectories of the waves labeled in Fig. 2. The earlier results with cyclic boundary conditions in the transverse directions<sup>11</sup> are shown as the

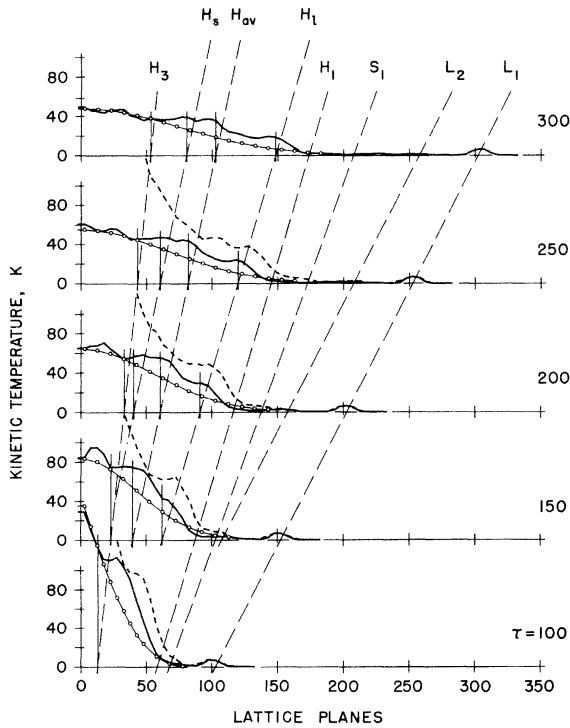


FIG. 3. Kinetic temperature ( $K$ ) vs lattice plane number, at several values of time  $\tau$ .  $T_i = 0$  K. Mirror boundary conditions (solid line), cyclic boundary conditions (dashed line), theoretical estimate of diffusive temperature profile (open circles). Long-dashed lines mark the progress of the various waves shown in Fig. 2 into the lattice.

broken curves. We note here that the energy of the system is not well conserved in this case: the total energy increased by a factor 1.56 in the interval from  $\tau = 100$  to  $\tau = 250$ . This energy increase was undoubtedly due to strain energy building up in the lattice because the cyclic boundary conditions allowed the filament to distort, as discussed in Sec. II. Changing to mirror boundary conditions has a dramatic effect: the total energy of the system now increases by only a factor 1.0006 in the interval from  $\tau = 100$  to  $\tau = 300$ . Despite the large difference in energy content, we note that the features identified by the dashed lines are inappreciably altered by changing the boundary conditions.

To delineate the heat pulse, we have plotted the diffusive contribution to heat flow, denoted by the open circles in this figure. This curve is determined by the finite difference method described in Sec. III. Our starting point is an approximately diffusive profile at  $\tau = 100$ . The diffusivity  $\alpha$  in the parameter  $z/2(\alpha\tau)^{1/2}$  is adjusted by trial and error to obtain a fit to the computed profile at  $\tau = 300$ . The fit is judged to be good when the heat pulse thus delineated does indeed lie between  $H_1$  and  $H_3$ , the beginning and end, respectively, of the heat pulse, over the entire time interval. The diffusive profile must also fit the boundary tem-

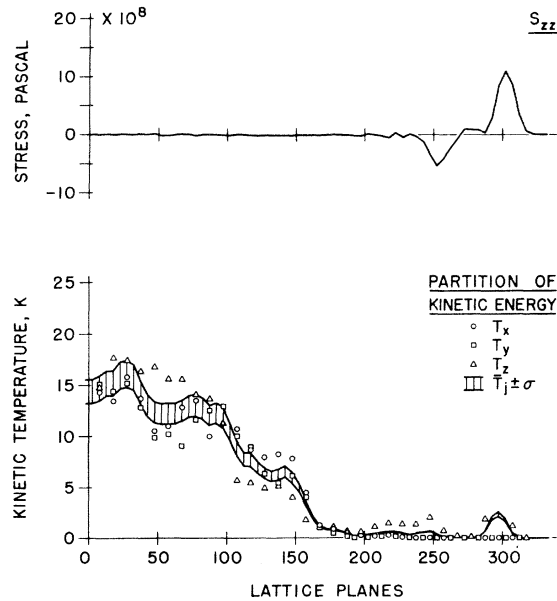


FIG. 4. Components of kinetic temperature  $T_j$  ( $K$ ) and longitudinal stress  $S_{zz}$  (Pascal) vs lattice plane number at  $\tau = 300$ . The points represent an average over 15 lattice planes and four time units:  $T_x$ ,  $\circ$ ;  $T_y$ ,  $\square$ ;  $T_z$ ,  $\triangle$ . The region with vertical bars shows the fluctuation in  $\bar{T}_j [= \frac{1}{3}(T_x + T_y + T_z)]$  for a standard deviation of  $\sigma = 0.0811$ .

perature, particularly at later times when we expect the flow to be diffusive. We see that these conditions are well satisfied by the curves in Fig. 3. The value of  $\alpha$  thus obtained is  $4.8 \times 10^{-6} \text{ m}^2 \text{ sec}^{-1}$ , in reasonable agreement with the earlier result for the two-dimensional lattice. The reason for choosing  $\tau = 100$  as a starting point rather than the more obvious choice of  $\tau = 40$  when heating ceases, is that the rapid cooling of the first ten planes causes the compressive potential energy due to the earlier heating to be converted into kinetic energy in those planes and, consequently, the boundary temperature rises as if heat were still being added to the system. Such a conversion is not accounted for in the diffusive theory. By  $\tau = 100$ , this conversion process is essentially complete.

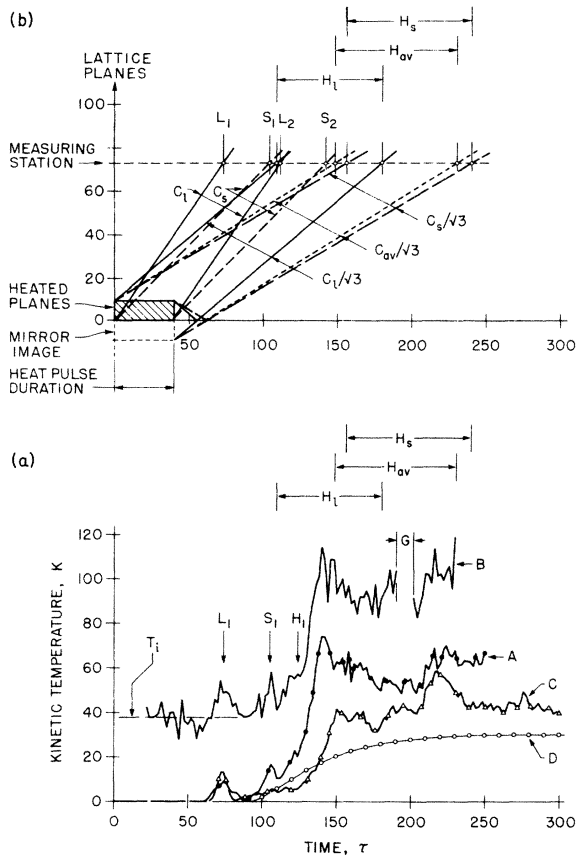


FIG. 5. (a) Kinetic temperature ( $K$ ) vs time  $\tau$  at station 15 in lattice (average of five planes from 71 to 75).  $G$  denotes gap in computer printout. (A) Cyclic boundary conditions, initial temperature of lattice,  $T_i = 0 \text{ K}$ ; (B) cyclic boundary conditions,  $T_i = 38 \text{ K}$ ; (C) mirror boundary conditions,  $T_i = 0 \text{ K}$ ; (D) theoretical estimate of diffusive profile. (b) Wavefront construction: plane number vs time, to show development of the various pulses. Ranges  $H_1$ ,  $H_{av}$ , and  $H_s$  mark the heat-pulse components. Labeling as in Fig. 2.

We now consider each of the wave features of Fig. 2 in turn. The pulses  $L_1$  and  $L_2$  travel with the velocity of longitudinal sound  $C_l$ , and their time of separation (50 units) is a little longer than the duration of heating. Figure 4 shows that they are longitudinal sound waves generated by the expansion on heating and contraction on subsequent cooling, respectively, of the boundary planes. There are, of course, some longitudinal waves within this interval and following it, due to the elastic coupling between the heated layers and the rest of the lattice. This produces a ringing effect. Longitudinal phonons are also produced during the period of steady heating. The shear waves generated by the expansion and contraction are very faint, but a small pulse  $S_1$  is discernible, traveling with the shear velocity  $C_s$ . In this region of stress pulses, we note that almost all the kinetic energy resides in the  $z$  component  $T_z$ , thus there is neither stress nor thermal equilibrium.

In the region between  $H_1$  and  $z = 0$ , Fig. 4 shows that not only is  $S_{zz}$  (and the other stress components) in equilibrium, but the components of kinetic temperature are also quite comparable. We use equilibrium theory to judge how close this region comes to local thermal equilibrium: we find the standard deviation ( $\sigma$ ) appropriate to a system consisting of the 15 planes ( $N = 303.75$  atoms) which contribute to one point in the figure to be  $\sigma = (2/N)^{1/2} = 0.0811$ , and use this value to obtain the fluctuation expected for one component of kinetic energy in a system in thermal equilibrium. The expected fluctuation is shown by the band of vertical lines in Fig. 4. In fact, this band should be wider for the  $x$  and  $y$  components, since the mirror boundary conditions reduce the effective number of atoms in 15 planes to 240 (i.e.,  $\sigma = 0.0913$ ). In the heat-pulse region, we see that nearly half the points lie within the acceptable band and a large majority of them lie within two standard deviations. For the few remaining points, the fluctuation is at most four standard deviations. This contrasts with the stress pulse region where the fluctuation is many times larger. We consider that these results show that local thermal equilibrium is well-enough attained in the heat-pulse region. Since  $H_1$  and  $H_s$  are straight lines (Fig. 3), we conclude that the temperature pulse superimposed on the diffusive background between  $H_1$  and  $H_s$  is propagating as a temperature wave. This temperature wave is a composite of the waves labeled  $H_1$ ,  $H_{av}$ , and  $H_s$ . These waves travel with velocity  $C_l/\sqrt{3}$ ,  $C_{av}/\sqrt{3}$ , and  $C_s/\sqrt{3}$ , respectively.  $C_{av}$  is the velocity defined by

$$C_{av}^2 = \frac{\sum_j C_j^{-3}}{\sum_j C_j^{-5}}$$

where  $C_j$  is the velocity of the  $j$ th mode, according to the theory of second sound in a Debye solid.<sup>17</sup> For our interatomic potential,

$$C_{av} = 0.731C_l \text{ and } C_s = 0.703C_l .$$

We note that although  $H_l$  travels at the same velocity as  $H_t$ , the apparent end of the pulse  $H_s$  trails behind  $H_s$  at a constant but slower velocity. This indicates that nondiffusive heat flow continues to be generated after heating at the boundary ceases, perhaps due to the ringing effect mentioned above.

From these results we conclude that  $H_l$  and  $H_s$  are the temperature waves associated with the initial disturbance which generates the longitudinal and transverse waves ( $L_l$  and  $S_l$ ) and that  $H_{av}$  comes from the period of steady heating of the boundary planes which produces an isotropic distribution of phonons. These temperature waves are analogous to the results of second-sound theory based on the Boltzmann transport equation for a phonon gas<sup>5</sup> or on the lattice response to a displacement field.<sup>6,7</sup> The main difference is that these theories treat the linearized small-perturbation problem where the thermal and elastic responses of the lattice are essentially uncoupled, whereas we treat the case of a large disturbance with strong thermoelastic coupling.

We now look at these waves from the standpoint of station 15 in the lattice, as shown in Fig. 5(a). First we note that all the features in (A)  $T_i = 0$  K are evident in (B)  $T_i = 38$  K, although at this moderately high temperature one would expect heat transfer to be by diffusion. The reason why we observe the heat pulse under these conditions is that we have sent a very strong heat pulse (800 K) into a comparatively short lattice. The pulse does not have time to damp away and disappear in thermal noise. Next, we note that the arrival times of each wave are the same in (A) and (B), and are thus independent of temperature, as we would expect since the longitudinal and transverse sound velocities,  $C_l$  and  $C_s$ , respectively, are approximately independent of temperature. Case (C) provides an example of changing the boundary conditions. We see that  $S_l$  is suppressed and the arrival time of the heat pulse is delayed. This result is reasonable since mirror boundary conditions restrict motion in the transverse directions, thereby inhibiting the formation of a shear stress pulse and the transfer of energy to the transverse modes. Such energy transfer is necessary for equilibration. The composite nature of the heat pulse is made quite clear in Fig. 5(b). Note that the pulses  $H_l$  and  $H_s$  should not have sharp cutoffs at long times because of the ringing effect mentioned earlier.

We now compare our results with the experimental results of McNelly *et al.*<sup>3</sup> We note that the computed profiles [Fig. 5(a)] are strikingly similar to those shown in Fig. 1(b) of Ref. 3, particularly that at  $T_i = 14.3$  K. Their "new" pulse corresponds to our heat pulse, and their first-sound waves  $L$  and  $T$  correspond to our  $L_l$  and  $S_l$  waves. At first sight the similarity is surprising in view of the vast differences between the two systems. For example, we have a perfect lattice model of  $\alpha$ -iron, they have a triply grown crystal of NaF; we use a strong heat pulse ( $\sim 800$  K), whereas they use a weak pulse ( $\sim 1$  K). The methods of heating and pulse detection are different as are both the time and distance scales (by a factor  $10^6$ ). However, we can understand the similarity by reference to the wave diagram shown in Fig. 5(b). There the wave velocities are normalized to the longitudinal velocity of sound, therefore this diagram, appropriately scaled, applies to the experimental system also. If we choose our measuring station (length of crystal) and heat-pulse duration to correspond to those in the heat-pulse experiments, then the temperature profile observed at the station [see Fig. 5(a)] should correspond to the experimental results [Fig. 1(b) of Ref. 3] provided that the relative damping of the waves also scales in some manner. That we do observe similar waves in the two systems means that this is indeed the case. This is an important result. However, in our present study we do not have a way of obtaining any quantitative information on the temperature and frequency dependence of the damping. This information is also lacking in the experiments as evidenced in the arbitrary scales for the temperature. On a qualitative basis, we draw the following conclusions: Damping is small for the first-sound waves because the wavelength of the heat pulse is long compared with the lattice spacing in both cases. Damping is small for our second-sound waves in spite of the high temperature, because of the extremely short time of propagation. Experimentally, damping is minimized by suitable choice of the conditions to reduce momentum nonconserving scattering processes (e.g., impurity and umklapp scattering) relative to momentum conserving processes (normal phonon scattering). That we see both second sound and diffusion indicates that our time of observation lies in between, or close to, the relaxation times for normal and umklapp scattering. Under these conditions, we conclude that there should be dynamic similarity between the model and experiment.

One aspect of the experimental results remains puzzling: Why are the  $L$  and  $T$  pulses so large? According to theory which treats a small temperature disturbance and neglects coupling to the

elastic equations of motion, the first-sound pulses associated with the second sound should have very small amplitudes. But the experiments show that, with a small disturbance, the first-sound pulses are of comparable amplitude to the heat pulse. These waves are presumed to be ballistic phonons which have reached the detector unscattered. Such a contribution to the pulse in our computer "experiment" would be swamped by the large stress pulse. Unfortunately, we do not know the experimental conditions in sufficient detail to understand the origin of these pulses. Such uncertainty does not arise in our case. We have applied a large disturbance to the system and can see that the first- and second-sound waves are of comparable magnitude. This results from the strong coupling between kinetic and potential energy in the system. We wish to emphasize that, regardless of their origin, in neither calculation nor experiment are the first-sound pulses in equilibrium, and time is needed for the process of equilibration.

On the basis of these considerations, we conclude that the heat pulse observed experimentally is a composite wave like ours. With this composite nature in mind, we next turn to the problem of the temperature dependence of the second-sound velocity shown in Fig. 2 of Ref. 3. In that figure, we see that the "new" pulse does not have a velocity corresponding to the wave  $H_{av}$  ( $V_{II}$  in their notation) according to theory.<sup>17</sup> Its velocity varies from  $C_s$  at the lowest temperature to approximately  $C_s/\sqrt{3}$  at the highest temperature of measurement. For NaF,  $C_s$  is approximately equal to  $C_1/\sqrt{3}$ , so we identify the new pulse at lowest temperatures with  $H_1$ . In the experimental results for  $T_i = 8.1$  K [see Fig. 1(b) of Ref. 3] a pulse is discernible at  $7 \mu\text{sec}$ . This corresponds to a wave with velocity  $C_s/\sqrt{3}$  which we identify with  $H_s$ . Thus we have experimental evidence of individual waves contributing to the heat pulse. We expect the apparent velocity of this heat pulse to vary with temperature. The exact shape and height of each component wave will be affected by the initial and boundary conditions, and by damping, so that the resultant pulse shape observed at a given station may vary as the components vary relative to each other. Indeed, we have seen the effect of changing the boundary conditions in our calculations [Fig. 5(a)]. Thus we conclude that the composite nature of the heat pulse may account for the observed temperature dependence of its arrival time. This interpretation is appealing in its simplicity and naturalness. It is certainly different from theoretical attempts to explain the temperature dependence of  $V_{II}$ .<sup>8</sup> Beck and Beck obtain a temperature dependence by using two temperature-dependent relaxation times in their

solution of the phonon Boltzmann equation. Ranning considers the energy-density and quasi-momentum-density correlation functions and obtains a temperature-dependent velocity from the dispersion relations for the possible modes in which energy fluctuations propagate, also assuming temperature-dependent relaxation times. In both theories,  $V_{II}$  is the maximum velocity at which second sound can propagate. However, we should point out that our explanation is somewhat tentative since we have carried out calculations for only two temperatures. We need further calculations and experiments using a strong heat pulse to establish our present understanding on a completely satisfactory basis.

As a final test of our model, we sent the heat pulse into a two-dimensional lattice at 0 K. Theory predicts that the second-sound velocity should be  $C_{av}/\sqrt{2}$  in this case. We show the kinetic temperature profiles in Fig. 6. We see the same features as in three dimensions save that the shear wave is not clearly resolved. The temperature waves  $H_1$ ,  $H_{av}$ , and  $H_s$  travel with velocity  $C_1/\sqrt{2}$ ,  $C_{av}/\sqrt{2}$ , and  $C_s/\sqrt{2}$ , respectively, where

$$C_{av}^2 = (C_s^{-3} + C_1^{-3}) / (C_s^{-5} + C_1^{-5})$$

or

$$C_{av} = 0.754C_1.$$

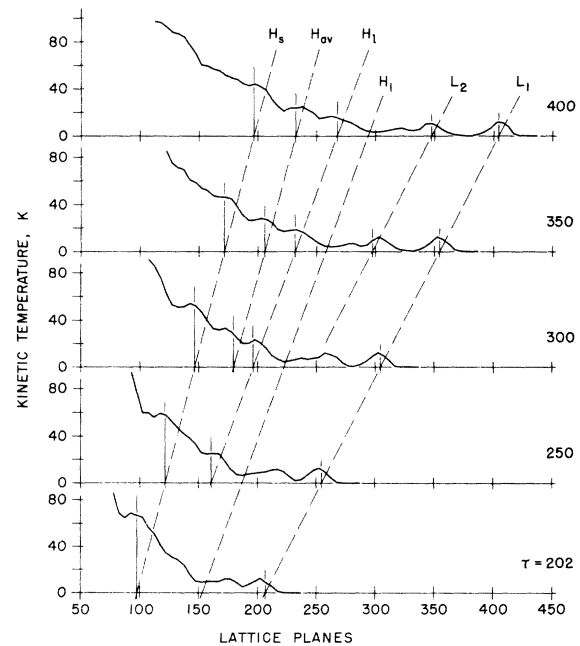


FIG. 6. Kinetic temperature ( $K$ ) vs lattice plane number at several values of time  $\tau$ .  $T_i = 0$  K, cyclic boundary conditions, two-dimensional lattice. Labeling as in Fig. 2.

### V. CONCLUSIONS

This study of an intense heat pulse propagating into a lattice has shown in great detail how the energy in the pulse is transported through the lattice. It is quite clear that the energy propagates as waves, superimposed on a diffusive background and we are able to link these waves with the initial conditions via the wave-front construction. We show that longitudinal and transverse stress waves, traveling with velocity  $C_l$  and  $C_s$ , respectively, are generated by the expansion of the boundary planes as they are rapidly heated. These waves are not in thermal equilibrium but they have temperature waves  $H_l$ ,  $H_s$  associated with them which travel with the appropriate second-sound velocity,  $C_l/\sqrt{3}$  or  $C_s/\sqrt{3}$ . The waves  $H_l$  and  $H_s$  combine with the wave  $H_{av}$  generated by the steady heating of the boundary layers, to form the composite wave  $H_l H_s$ . We show that this wave corresponds to the heat pulse observed in low-temperature second-sound experiments. Because of its composite nature, the shape, height, and velocity of this wave may vary as the component waves vary relative to one another upon change of the initial and boundary conditions. In this way we can understand the temperature dependence of the heat-pulse arrival time observed experimentally. The idea of a longitudinal (transverse) second sound associated with longitudinal (transverse) first sound is not new, it is evident in the theory of interacting phonons based on the atomic displacement correlation function<sup>6,7</sup> but it has not been looked for in experiments, perhaps because the amplitude is expected to be very small, as discussed in the previous section. This leads us to the relation between these results and our earlier work on shock wave propagation where we observed that the thermally equilibrated region behind the shock front propagated at roughly the velocity of longitudinal second sound. This is essentially the same situation as the longitudinal first-sound wave  $L_1$  and its associated second-sound wave  $H_1$ . The second-sound velocity is somewhat slower than the expected  $C_{\text{shock}}/\sqrt{3}$  owing to dispersion, which is important here since the shock front contains predominantly slow high-frequency phonons.

We wish to emphasize one point which is central to our understanding of the relaxation problem in

a solid. That is the distinction between thermalized (equilibrated) and nonthermalized energy disturbances. First sound shows itself as a stress pulse which disturbs the potential and kinetic energies of the lattice locally, but the pulse is not thermalized. Second sound, on the other hand, is by definition a thermalized wave, and since the relaxation process in strongly coupled systems involves the thermal equilibration of both kinetic and potential energies, it takes time to establish thermal equilibrium. Consequently, a temperature wave cannot travel as fast as first sound. This is in contrast to the situation in a simple gas, where there is essentially no coupling (no potential energy) so thermal equilibrium is attained very rapidly.

To sum up our results, this study of the strong heat pulse has enabled us to extend the realm of second sound to high temperatures and high pressures, and consequently to the strongly anharmonic system, thereby increasing our understanding of the general problem of thermal relaxation in a solid. We find that coupling between the elastic and thermal response of the system is important and that our model is able to give a satisfactory account of this coupling. In spite of vastly different conditions, we are able to relate our results to the usual low temperature and weak heat-pulse experiments because of the dynamical similarity between our model and the experimental situation. At present, the molecular-dynamical method appears to provide the only practical means for studying closely coupled systems subjected to strong disturbances. We hope this work will encourage experimental work to be done in this regime.

### ACKNOWLEDGMENTS

We thank Dr. Max Klein, Chief of the Equation of State Section, for his encouragement and helpfulness in the course of this work. We appreciate several discussions with Professor J. A. Krumhansl and Professor P. G. Klemens regarding the theory of second sound. We also thank Dr. J. O'Keefe and E. Sullivan of the Theoretical Division of the Goddard Space Flight Center, Greenbelt, Md. for enabling us to use the computer at Greenbelt for some of our calculations.

\*Work performed with partial support from the U.S. ERDA under Interagency Agreement No. AT(49-13)3003, and from the U.S. ARO under Contract No. MIPR ARO 3-76.

<sup>1</sup>B. J. Alder and T. E. Wainwright, *J. Chem. Phys.* **33**,

1439 (1960); A. Rahman, *Phys. Rev.* **136**, A405 (1964); L. Verlet, *ibid.* **159**, 98 (1967); **165**, 201 (1968).

<sup>2</sup>D. N. Payton, M. Rich, and W. M. Visscher, *Phys. Rev.* **160**, 706 (1967); E. A. Jackson, J. R. Pasta, and J. F. Waters, *J. Comp. Phys.* **2**, 207 (1968); W. T. Ashurst

- and W. G. Hoover, *Phys. Rev. A* **11**, 658 (1975).
- <sup>3</sup>T. F. McNelly, S. J. Rogers, D. J. Channin, R. J. Rollefson, W. M. Goubau, G. E. Schmidt, J. A. Krumhansl, and R. O. Pohl, *Phys. Rev. Lett.* **24**, 100 (1970).
- <sup>4</sup>C. C. Ackerman, B. Bertman, H. A. Fairbank, and R. A. Guyer, *Phys. Rev. Lett.* **16**, 789 (1966); C. C. Ackerman and W. C. Overton, *ibid.* **22**, 764 (1969); V. Narayanamurti and R. C. Dynes, *ibid.* **28**, 1461 (1972).
- <sup>5</sup>J. C. Ward and J. Wilks, *Philos. Mag.* **43**, 48 (1952); E. W. Prohofsky and J. A. Krumhansl, *Phys. Rev.* **133**, A1403 (1964); R. A. Guyer and J. A. Krumhansl, *ibid.* **133**, A1411 (1964); **148**, 766 (1966).
- <sup>6</sup>P. C. Kwok and P. C. Martin, *Phys. Rev.* **142**, 495 (1966).
- <sup>7</sup>L. Sham, *Phys. Rev.* **156**, 494 (1967); **163**, 401 (1967).
- <sup>8</sup>J. Ranninger, *Phys. Rev. B* **5**, 3315 (1972); H. Beck, and R. Beck, *ibid.* **8**, 1669 (1973).
- <sup>9</sup>D. H. Tsai, *Accurate Characterization of the High Pressure Environment*, edited by E. C. Lloyd, Natl. Bur. Stds. (U.S.) Spec. Publ. No. 326 (U.S. GPO, Washington, D.C., 1971), p. 105.
- <sup>10</sup>D. H. Tsai and R. A. MacDonald, *J. Phys. C* **6**, L171 (1973).
- <sup>11</sup>D. H. Tsai and R. A. MacDonald, *Solid State Commun.* **14**, 1269 (1974).
- <sup>12</sup>R. A. MacDonald and D. H. Tsai, *Thermal Conductivity 14*, edited by P. G. Klemens and T. K. Chu (Plenum, New York, 1976), p. 145.
- <sup>13</sup>R. Chang, *Philos. Mag.* **16**, 1021 (1968).
- <sup>14</sup>P. J. Schneider, *Conduction Heat Transfer* (Addison-Wesley, Cambridge, 1955), pp. 272-276.
- <sup>15</sup>C. Y. Ho, M. W. Ackerman, K. Y. Wu, S. G. Oh, and T. N. Havill, Purdue University, T.P.R.C. Report No. 30 (1975) (unpublished).
- <sup>16</sup>M. Jakob, *Heat Transfer* (Wiley, New York, 1959), pp. 383-385.
- <sup>17</sup>J. A. Sussmann and A. Thellung, *Proc. Phys. Soc. Lond.* **81**, 1122 (1963).